different updating timings for both amplitude- and phase-based updating approaches. Several metrics, including target coverage, duty cycle, residual motion in the gating window, residual error for all false positives, are defined to evaluate gated treatment.

The results showed that dynamic correlation updating is necessary for the success of gated radiation treatment. Moreover, gated treatment has high requirements for the timing of correlation updates, i.e., correlation updating near the gating window entry point improves more for the average target coverage, with some sacrifice of treatment efficiency. This is the major difference between our updating algorithms and other correlation updating methods (Kanoulas *et al* 2007). One update per breathing cycle (~0.2 Hz for internal imaging) is acceptable for most regular treatments with improved target coverage. For long lasting treatments, internal imaging can be further reduced by a factor of two, i.e., one update every two breathing cycles, with the sacrifice of a couple of percentages of target coverage (1.65%). Compared to the RTRT system with an internal imaging rate of 30 Hz, our approach has reduced the internal imaging dose more than 150 times. The residual errors in the gating window or for all false positive showed that our updating algorithms reduce residual motion and lower false positive rate.

Further investigation is being carried out to study gating based on updated internal/external signals in a clinical environment. For example, one direction is to integrate advanced features, such as the estimation of motion uncertainties and phase discrepancies during internal imaging, and the impact of motion hysteresis, into the correlation updating algorithm. Another direction is the simulation of gating during a real-time treatment with motion prediction by considering the system delay and imaging rate (Sharp *et al* 2004). Yet another direction is to integrate the updating algorithms to dynamically change the sizes and positions of the gating window under the restrictions of treatment planning system. It will be very useful for patients with irregular motion, especially with baseline drift. In addition, more precise evaluation metrics for gating are under active exploration.

References

Berbeco R I, Mostafavi H, Sharp G C and Jiang S B 2005a Towards fluoroscopic respiratory gating for lung tumours without radiopaque markers *Phys. Med. Biol.* **50** 4481–90

Berbeco R I, Nishioka S, Shirato H, Chen G T Y and Jiang S B 2005b Residual motion of lung tumours in gated radiotherapy with external respiratory surrogates *Phys. Med. Biol.* **50** 3655–67

Bortfeld T, Jokivarsi K, Goitein M, Kung J and Jiang S B 2002 Effects of intra-fraction motion on IMRT dose delivery: statistical analysis and simulation *Phys. Med. Biol.* **47** 2203–20

Chui C S, Yorke E and Hong L 2003 The effects of intra-fraction organ motion on the delivery of intensity-modulated field with a multileaf collimator *Med. Phys.* **30** 1736–46

Cui Y, Dy J G, Sharp G C, Alexander B and Jiang S B 2007 Robust fluoroscopic respiratory gating for lung cancer radiotherapy without implanted fiducial markers *Phys. Med. Biol.* **52** 741–55

Han J and Kamber M 2000 *Data Mining Concepts and Techniques* 2nd edn (New york: Morgan Kaufmann)

Ionascu D, Jiang S B, Nishioka S, Shirato H and Berbeco I R 2007 Internal–external correlation investigations of respiratory induced motion of lung tumors *Med. Phys.* **34** 3893–903

Jiang S B 2006 Radiotherapy of mobile tumors *Semin. Radiat. Oncol.* **16** 239–48

Jiang S B, Pope C, Aljarrah K M, Kung J, Bortfeld T and Chen G T Y 2003 An experimental investigation on intra-fractional organ motion effects in lung IMRT treatments *Phys. Med. Biol.* **48** 1773–84

Kanoulas E, Aslam J A, Sharp G C, Berbeco R I, Nishioka S, Shirato H and Jiang S B 2007 Derivation of the tumor position from external respiratory surrogates with periodical updating of the internal/external correlation *Phys. Med. Biol.* **52** 5443–56

Keall P J, Kini V R, Vedam S S and Mohan R 2002 Potential radiotherapy improvements with respiratory gating *Australas. Phys. Eng. Sci. Med.* **25** 1–6

Korreman S, Christensson J, Mostafavi H, Loo B, Le Q and Boyer A 2007 Predictability of lung tumor motion based on external marker monitoring: linear and non-linear modelling *Proc. ICCR*

Kubo H D and Hill B C 1996 Respiration gated radiotherapy treatment: a technical study *Phys. Med. Biol.* **41** 83–91

Murphy M J 2004 Tracking moving organs in real time *Semin. Radiat. Oncol.* **14** 91–100
Schweikard A *et al* 2000 Robotic motion compensation for respiratory movement during radiosurgery *Comput. Aided. Surg.* **5** 263–77
Seppenwoolde Y, Berbeco R I, Nishioka S, Shirato H and Heijmen B 2007 Accuracy of tumor motion compensation algorithm from a robotic respiratory tracking system: a simulation study *Med. Phys.* **34** 2774–84
Sharp G C, Jiang S B, Shimizu S and Shirato S 2004 Prediction of respiratory tumour motion for real-time image-guided radiotherapy *Phys. Med. Biol.* **49** 425–40
Shirato H *et al* 2000 Four-dimensional treatment planning and fluoroscopic real-time tumor tracking radiotherapy *Int. J. Radiat. Oncol. Biol. Phys.* **48** 1187–95
van Herk M 2004 Errors and margins in radiotherapy *Semin. Radiat. Oncol.* **14** 52–64
Vedam S S, Keall P J, Kini V R and Mohan R 2001 Determining parameters for respiration-gated radiotherapy *Med. Phys.* **28** 2139–46
Wu H, Sharp G, Salzberg B, Kaeli D, Shirato H and Jiang S 2004 A finite state model for respiratory motion analysis in image guided radiation therapy *Phys. Med. Biol.* **49** 5357–72

Jpn J Clin Oncol 2008;38(7)486–492
doi:10.1093/jjco/hyn049

Low-dose Craniospinal Irradiation and Ifosfamide, Cisplatin and Etoposide for Non-metastatic Embryonal Tumors in the Central Nervous System

Koichi Yasuda[1], Hiroshi Taguchi[1], Yutaka Sawamura[2], Jun Ikeda[2], Hidefumi Aoyama[1], Kenji Fujieda[3], Nobuaki Ishii[2], Masaaki Kashiwamura[4], Yoshinobu Iwasaki[2] and Hiroki Shirato[1]

[1]Department of Radiology, Hokkaido University School of Medicine, [2]Department of Neurosurgery, Hokkaido University School of Medicine, [3]Department of Pediatrics, Hokkaido University School of Medicine and [4]Department of Otolaryngology, Hokkaido University School of Medicine, Sapporo, Japan

Received February 5, 2008; accepted May 26, 2008; published online June 23, 2008

Objective: The current study was conducted to evaluate the effects of low-dose craniospinal irradiation (CSI) combined with chemotherapy on non-metastatic embryonal tumors in the central nervous system (CNS), including medulloblastoma and supra-tentorial primitive neuroectodermal tumors (ST-PNET).
Methods: All patients were treated according to the following protocol. After surgery, the patients ≤5 years old received 18 Gy and the patients >5 years old received 24 Gy CSI. The dose to the primary tumor bed was 39.6–54 Gy. Chemotherapy consisted of ifosfamide, cisplatin and etoposide (ICE chemotherapy).
Results: Sixteen patients aged 0.5–20.4 (median 6.1) years were enrolled and followed for 11–165 (median 112) months. Both 5-year actuarial overall survival (OAS) and progression-free survival (PFS) were 81% (95% confidence interval (CI): 62–100%) for the 16 patients. Both 5-year OAS and PFS were 82% (CI: 59–100%) for the patients with medulloblastoma and 80% (CI: 45–100%) for the patients with ST-PNET. Both 5-year OAS and PFS were 75% for the eight patients ≤5 years old and 88% for the eight patients >5 years old. Both 5-year OAS and PFS were 100% for six average-risk patients (3 years or older, total resection and posterior fossa) and 70% for 10 poor-risk patients (others). The median total intellectual quotient at the last follow-up was 85 (ranging from 48 to 103) in 12 patients who were followed for 3–145 (median 49) months. Eight patients received hormone replacement therapy.
Conclusion: Low-dose CSI and ICE chemotherapy may have a role as a treatment option for a subset of patients with non-metastatic embryonal tumors in the CNS.

Key words: medulloblastoma – primitive neuroectodermal tumor – chemotherapy – radiotherapy – late effect

INTRODUCTION

The standard therapy for medulloblastoma has been 35–36 Gy craniospinal irradiation (CSI) and 54–55.8 Gy to the tumor bed after surgical resection (1). A recent randomized trial has shown that a combination of pre-radiotherapy intensive chemotherapy and 35 Gy CSI was significantly better in outcome than 35 Gy CSI alone for non-metastatic medulloblastoma in terms of event-free survival and possibly overall survival (OAS) (2). However, since CSI has produced neuro-cognitive dysfunction and endocrine deficiency in young children and infants (3), dose reduction in CSI with or without chemotherapy has been tested. A total of 25 Gy of CSI was associated with the poorer outcomes in multi-institutional phase III trials with or without chemotherapy (4,5). Subset analysis, however, showed that for patients treated with radiotherapy alone, event-free survival at

Presented in part at the 49th annual meeting of the American Society of Therapeutic Radiology and Oncology in October 2007.

For reprints and all correspondence: Koichi Yasuda, Hokkaido University School of Medicine, North-15 West-7, Kita-ku, Sapporo, Japan.
E-mail: kyasuda@rndi.med.hokudai.ac.jp

5 years was identical between 25 and 35 Gy CSI (4). Pilot studies and a multi-institutional phase II study suggested that 23.4–30 Gy CSI with pre- or post-radiation chemotherapy could achieve similar results with standard-dose CSI for average-risk medulloblastoma (6–8). Important questions remain with respect to the radiotherapy dose in CSI for medulloblastoma. To reduce the incidence of the late adverse effects of CSI, we performed a prospective protocol study using reduced-dose CSI sandwiched between chemotherapy that consisted of an ifosfamide, cisplatin and etoposide (ICE) regimen.

Patients with supra-tentorial primitive neuroectodermal tumors (ST-PNET) have clinical features different from those with medulloblastoma (9–12). However, these two diseases were categorized as the embryonal tumors in the WHO classification of brain tumor (9). Because of the similarity in pathological features, these two diseases have been often treated similarly (13,14). We have also determined the treatment strategy for ST-PNET to be similar to that of medulloblastoma with regard to maximal surgical resection, intensive chemotherapy and radiotherapy. Patients with ST-PNET were also entered and evaluated in this study.

In this study, we have evaluated long-term outcome, both in survival and adverse effect of patients with non-metastatic medulloblastoma and ST-PNET, or embryonal tumors in the central nervous system (CNS).

MATERIALS AND METHODS

Selection Criteria

Entry criteria for patients were as follows: the age between 6 months and 30 years, and with histologically proven medulloblastoma or ST-PNET. The patients or guardians had to give informed consent prior to surgery and again prior to adjuvant therapy.

Treatment

The flow chart of the treatment strategy is shown in Fig. 1.

Total surgical resections were attempted in patients with medulloblastoma who had Chang's Stage T1, T2 or T3a without evidence of metastasis (Stage M0) (15). Brainstem origin tumors were biopsied or partially removed. Patients with ST-PNET without evidence of metastasis were also treated at first with maximum surgical resection. Ventriculostomy, but not venticuloperitoneal shunting, was performed at tumor removal in patients with hydrocephalus.

Patients with either medulloblastoma or ST-PNET received ICE chemotherapy and CSI with a generous local boost to the tumor site (16). The ICE regimen consisted of three agents; ifosfamide at 900 mg/m^2 (Days 1–5), cisplatin at 20 mg/m^2 (Days 1–5) and etoposide at 60 mg/m^2 (Days 1–5) every 4 weeks. To prevent hemorrhagic cystitis and to suppress emesis, sodium 2-mercaptoethane sulfonate (810 mg/m^2/day) and granisetron hydrochloride (40 or 80 mg/kg/day), a 5-hydroxy-tryptamine receptor antagonist, were intravenously administered from Day 1 to 5. Hydration, including the infusion of mannitol, was done routinely.

In principle, the ICE chemotherapy regimen should have begun within 2 weeks of the surgery. The intent was for the ICE chemotherapy regimen to begin within 2 weeks of the surgery, but this did not always occur, as the timing of the chemotherapy and radiotherapy varied. Patients <2.5 years old received eight cycles of chemotherapy every 4 weeks and then received 18 Gy CSI and a local boost of 30–36 Gy when they became 2.5 years old. For patients between 2.5 and 5 years old, one course of ICE followed by 18 Gy CSI and a local boost of 30–36 Gy were scheduled. For patients <5 years old, one course of ICE followed by 24 Gy CSI and a local boost of 30 Gy were scheduled. Thus, the irradiation dose to the hypophysis and hypothalamus was 18 Gy for patients 5 years old or younger and 24 Gy (20–30) for patients >5 years in medulloblastoma. For patients with ST-PNET, the dose to the hypophysis and hypothalamus was distributed from 18 to 38 Gy.

After the radiotherapy, up to six cycles of ICE was administered to the patients 2.5 years old or older. The intent was for patients to receive CSI immediately followed by the local tumor boost, but if myelosuppression had been prolonged by the ICE before radiotherapy, they received local irradiation first, followed by CSI.

Whole-brain irradiation was performed using nearly parallel-opposed lateral fields with multi-leaf collimators to block the lenses of both eyes and including all cerebrospinal fluid space. Whole-spinal irradiation was performed using posterior single or two serially arranged posterior fields including all cerebro-spinal fluid space leaving the patient in the same position on the table. Dose distribution was calculated using a three-dimensional radiotherapy planning

Figure 1. Flow chart of the treatment strategy. ICE chemotherapy, ifosfamide, cisplatin and etoposide; CSI, craniospinal irradiation

system. The radiotherapy dose was prescribed at the center of the midline for the whole brain and at the mean depth of the spinal canal. The boost to the posterior fossa in medulloblastoma and to the tumor bed in ST-PNET was performed using two angled and wedged fields to reduce the dose to the ear structures, temporal and posterior lobes for medulloblastoma. In patients treated in the latter half of the study period, three or more non-coplanar fields were used to reduce unnecessary dose to the surrounding structures. Daily fractions of 1.8–2.0 Gy were used at the isocenter.

Toxicity-related Dose Adjustment for the ICE Regimen

All patients underwent urological and audiological examination and renal monitoring before each cycle of chemotherapy. The chemotherapy doses were modified if there was any evidence of hematological, renal or audiological toxicity according to the dose-reduction criteria (16). If the creatinine clearance was $<70\%$, cisplatin was omitted for that cycle and only given thereafter if renal or hearing function improved. Routine urological examination was performed from Day 1 to 5 in each cycle. Ifosfamide was omitted if macrohematuria was observed and was begun again when microscopic hematuria disappeared. Etoposide and ifosfamide were reduced according to the myelosuppression score consisting of the blood count nadir and symptoms related to the previous course of ICE (16). The score was cumulative overall courses. When using this method, the next cycle would be omitted if the score was higher than anticipated for a long time without recovery.

Follow-up

Patients were followed-up by regular clinical examination. The follow-up intervals after the end of the treatment were every month in the first year, every 3 months in the second year, every 4 months in the third year and subsequently every 6 months. Repeat cranial MRIs with or without spinal MRI were performed every 3 months in the first year and every 6 months in the second to fifth years. After that, the follow-up was performed annually at our institution or at local hospitals.

Statistical Methods

The final analysis was performed in March 2007. OAS and PFS were analyzed. OAS was calculated as the time from the date of surgical diagnosis to the date of death. Patients still alive were censored at date last seen. Subjects with average risk included children >3 years of age with posterior fossas and those with tumors that were totally or 'nearly totally' (≤ 1.5 cc of residual disease) resected. Subjects with poor risk included children <3 years of age and/or those with subtotal resection ((1.5 cc's residual disease) and/or a non-posterior fossa location, including supra-tentorial location (10,11,12,17,18).

PFS was calculated as the time from the date of surgery to the date of recurrence or death. In those cases where death followed recurrence, the date of recurrence was used. Kaplan–Meier survival curves were produced, and log-rank tests were performed to compare OAS. Greenwood's formula was used to calculate the standard errors, which were then used to calculate the CI. The *t*-test was used to compare the interval between surgery and radiotherapy between groups.

RESULTS

Sixteen patients aged 0.5–20.4 (median 6.1) years were enrolled and followed for 11–165 months with a median of 112 months. The characteristics of the patients are listed in Table 1. In total, both the 5-year actuarial OAS and PFS were 81% (95% confidence interval, CI: 62–100%) for the 16 patients (Fig. 2). Both 5-year OAS and PFS were 82% (CI: 59–100%) for patients with medulloblastoma and 80% (CI: 45–100%) for patients with ST-PNET. The 5-year OAS and PFS were both 100% (CI: 100–100%) for the six average-risk patients and 70% (CI: 42–98%) for the 10 high-risk patients (Fig. 3). There was no statistical difference between the two groups (OAS: $P = 0.35$; PFS: $P = 0.26$). OAS and PFS were 81% (CI: 62–100%) and 68% (CI: 44–99), respectively, at 7 years, and were 74% (CI: 53–96%) and 68% (CI: 44–99%), respectively, at 9 years.

All eight patients ≤ 5 years of age received 18 Gy CSI. One of these eight patients (No. 10) experienced dissemination of the disease at 11 months after surgery and died at 16 months after surgery. Another patient (No. 11) who underwent a biopsy followed by three courses of chemotherapy and radiotherapy died at 11 months after biopsy without disappearance of the disease. The other six patients are alive at 117–months after surgery without evidence of disease. The 5-year OAS and PFS for the eight patients were both 75% (CI: 45–100%).

In the eight patients >5 years old, 24 Gy CSI was given to six patients. The CSI was stopped at 20 Gy due to severe myelosuppression in one patient (No. 4), and an additional 6 Gy (i.e. 30 Gy CSI) was given to another patient (No. 7) because of a strong fear that surgery would disseminate the disease. The 5-year OAS and PFS for the eight patients were both 88% (CI: 65–100%). Local relapse was observed in two patients, and dissemination disease was observed in one patient. All patients received 24 Gy CSI. One of them was rescued by high-dose chemotherapy with stem cell transplantation and lived for 44 months after the diagnosis of relapse. There was no statistical difference between patients ≤ 5 years and patients >5 years of age (OAS: $P = 0.51$; PFS: $P = 0.69$).

The total amounts of chemotherapeutic agents are listed in Table 2. Because we used reduction criteria for each agent in each cycle of the treatment, the total amount of chemotherapeutic agent varied. Two patients experienced relapse of the local tumor during chemotherapy, and the treatment was

Table 1. The characteristics of patients

No.	Sex	Age (years)	Primary	T	Risk	Surgery	Interval (days)	CSI (Gy)	Local (Gy)	TTT (days)	Relapse (months × 1)	Survival (months × 1)	Status	Adverse effects (months × 2)	IQ(initial) × 3	IQ (last follow-up) × 4
1	M	0.5	Cerebellum	T2	High	Partial	584	18	39.6	63		127	Alive	Growth hormone deficiency (38) Thyroid hormone deficiency (18) Radiation-induced hemangioma (53)	92	100
2	M	1	Cerebellum	T3b	High	NT	275	18	48	125		165	Alive		98	74
3	F	5	Cerebellum	T2	Low	NT	45	18	48	245		143	Alive		101	92
4	M	7.2	Cerebellum	T2	Low	NT	21	20	50	53		103	Alive	Thyroid hormone deficiency (31)	103	—
5	M	7.6	Cerebellum	T2	Low	NT	40	24	50	43	Local (76)	120	Dead	Corticosteroid deficiency (82) Thyroid hormone deficiency (49)	85	78
6	F	8.8	Cerebellum	T2	Low	Total	6	24	54	45		95	Alive	Thyroid hormone deficiency (12)	94	96
7	F	12.6	Cerebellum	T3a	Low	Total	37	30	54	49		113	Alive	Thyroid hormone deficiency (33)	68	73
8	M	20.4	Cerebellum	T2	Low	Total	7	24	50	255		111	Alive		—	—
9	F	1.2	4th ventricle	T3a	High	Total	22	18	46	40		134	Alive	Growth hormone deficiency (38) Antidiuretic hormone (ADH) deficiency (36)	79	—
10	M	1.9	4th ventricle	T3a	High	NT	262	18	50	52	Dissemin. (11)	16	Dead		—	—
11	F	2.5	pons	T3b	High	Biopsy	64	18	54	47	Local (0)	11	Dead		—	—
12	M	1.6	lt. parietal	—	High	NT	47	18	48	42		117	Alive		103	86
13	F	2.5	lt. parietal	–	High	NT	64	18	50	64		134	Alive	Corticosteroid deficiency (57) Thyroid hormone deficiency (63) Gonadotropin deficiency (115)	58	48
14	F	10.5	rt occipital	—	High	NT	22	24	54	45	Dissemin. (72)	88	Dead	Thyroid hormone deficiency (35)	—	—
15	F	12.3	rt. temporal	—	High	NT	28	24	54	49	Local (22)	28	Dead		85	—
16	M	14.3	rt occipital	—	High	NT	33	24	54	55		70	Alive		85	—

T, T stage; Interval, interval between surgery and radiotherapy; NT, nearly total resection; CSI, cerebrospinal irradiation dose; Local, local total irradiation dose; TTT, total treatment time; dissemin., dissemination; months × 1, months from surgical diagnosis; months × 2, months from the completion of all therapy at the onset of the disease or the start of hormonal supplement; IQ(initial) × 3, IQ score for the first time; IQ(last follow-up) × 4, IQ score at the last follow-up if IQ test was conducted more than once.

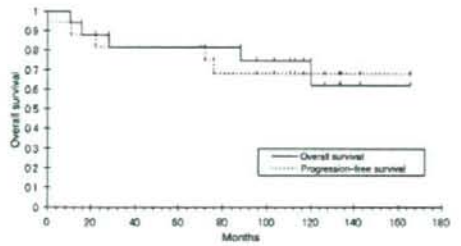

Figure 2. Overall and progression-free survival curves for 16 patients with non-metastatic embryonal tumors in the central nervous system.

stopped after three courses. The regimen of chemotherapy was changed in one patient after relapse, and a salvage operation was performed in another patient for the relapsed tumor.

Total intellectual quotient (IQ) was measured in 12 patients with the follow-up period ranging from 3 to 145 months with a median of 49 months (Fig. 4, Table 1). The median total IQ at the last follow-up was 85 (ranging from 48 to 103). In nine patients who were able to undergo the examination for verbal IQ (VIQ) and performance IQ (PIQ), there was no apparent discrepancy between VIQ (median 82, 95%CI: 48–119%) and PIQ (92, 58–113%) ($P = 0.75$). In eight patients whose total IQ was measured more than twice during the follow-up (median follow-up 78, 19–145%), two patients, whose latest IQ scores were 74 and 86, respectively, showed apparent deterioration in total IQ of >10 points (−24 and −17 points).

Eight patients received hormone replacement therapy because of deficiencies in thyroid hormone, corticosteroid hormone, growth hormone, antidiuretic hormone or gonadotropin (seven, two, two, one and one patients, respectively). Irradiated dose to the hypophysis and hypothalamus of the eight patients were 18–32 Gy (median 22 Gy). Two of the eight patients had ST-PNET.

No patients suffered from symptomatic hearing deficiency or required hearing aids. One patient experienced hemangioma in the skull in the irradiated region 4.4 years at the region which received 18 Gy and underwent surgical removal of the tumor.

Table 2. The nominal cycles of chemotherapy and the actual amount of chemotherapeutic agents

No.	Nominal cycles	Ifosfamide	Cisplatin	Etoposide
1	8	6.7	8	6.25
2	7	6.66	7	7
3	8	8	8	8
4	7	1.75	6	5.4
5	8	2	8	8
6	6	1	6	6
7	6	2.35	5.25	4.95
8	6	6	5	6
9	8	6.05	7	6.05
10	7	5.85	6	6
11	3[1]	3	3	3
12	8	4.45	5.45	6
13	8	3.95	7.2	7.2
14	6	1.75	5	4.75
15	3[1]	2.35	2.75	2.35
16	6	2.95	6	6

The dose of each agent is shown in respect of the dose for one cycle.
[1]Stopped due to relapse during the treatment.

DISCUSSION

For medulloblastoma, the results of a multi-institutional study confirmed that low-dose CSI cannot be justified with or without chemotherapy (4,5). However, the possibility of serious late complications related to radiotherapy after standard-dose CSI suggests that we should investigate better treatment options with less morbidity. Packer et al. (6) have shown that reduced-dose craniospinal radiation therapy (23.4 Gy) followed by adjuvant chemotherapy of lomustine 75 mg/m^2, vincristine 1.5 mg/m^2 and cisplatin 75 mg/m^2 for average-risk patients can achieve PFS of 79 ± 7% at 5 years for average-risk medulloblastoma. Recently, Packer et al. have conducted a phase III trial for average-risk patients in which they compared the adjuvant chemotherapy described above

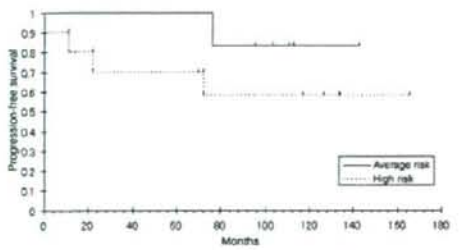

Figure 3. Progression-free survival curves for six patients with average risk and 10 patients with high risk of non-metastatic embryonal tumors in CNS.

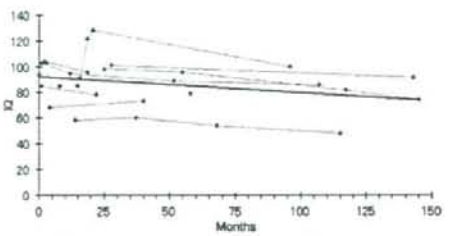

Figure 4. Temporal change of total intellectual quotient for 12 measurable patients with the regression line.

with a therapy in which cyclophosphamide was substituted for lomustine with the same low-dose craniospinal radiation therapy (23.4 Gy). They found that either choice of chemotherapy resulted in similar event-free survival rates: 82 ± 2.8% for chemotherapy with lomustine and 80% ± 3.1% for that with cyclophosphamide (19). Gajjar et al. (20) performed a prospective study of risk-adapted radiotherapy followed by chemotherapy in children with average-risk and high-risk medulloblastoma. In their analysis, 5-year event-free survival was 83% (73–93%) for the average-risk group, which received 23.4 Gy craniospinal radiotherapy, and 70% (55–85%) for the high-risk group, which received a conventional dose of 36–39.6Gy. They compared decreases in IQ and found that the difference between the low-dose craniospinal radiotherapy group and the conventional dose group was not statistically significant ($P = 0.097$) (21). The present study was consistent with their studies, showing similar survival rates and a moderate decrease in IQ. The reduced-dose CSI and chemotherapy may be as effective as standard CSI in terms of tumor control and neuro-cognitive function in long-term follow-up.

The combination of 18 Gy CSI and chemotherapy has been tested in 10 patients in a previous clinical trial, and seven of the 10 patients survived >5 years (22). Six out of eight patients ≤ 5 years old received 18 Gy CSI and survived >9 years in the present study. If we combine our results involving eight patients with these 10 patients in the literature, 13/18 survived longer than 5 years. The 5-year survival rate is not inferior to the previous results obtained with a higher CSI dose. However, Jakacki et al. (23) have reported that the administration of 1800 cGy CSI with chemotherapy to seven patients aged from 20 to 64 months was not advisable because of the high recurrence rate. Again, the number of patients was too small to exclude the possibility of a bias.

The superiority of low-dose CSI to conventional CSI for the purpose of reducing the late adverse effects remains a subject of debate (24,25). A full-scale IQ <80 was reported to be observed even in children with brain tumors who received irradiation only at the posterior fossa (26). Oyharcabal-Bourden et al. (27) have shown that the median total IQ in the follow-up was reported to be 83, and hormone replacement therapy was required in 41.9% of the patients who received adjuvant chemotherapy followed by 25 Gy craniospinal radiation therapy. Our results, which included a median total IQ of 85 and a requirement of hormone replacement therapy in 50% of the patients, were highly consistent with their study.

Treatment outcome of patients with ST-PNET has been reported to be poorer than that of those with medulloblastoma (10–11), and thus patients with ST-PNET are now treated with intensive chemotherapy in clinical trials (12). Because of the cerebral location of ST-PNET, the neuro-cognitive function is usually much poorer in these patients than in those with medulloblastoma. Our series is too small to be compared with the previous larger series, but the treatment outcome was comparable to other poor-risk patients with medulloblastoma. Careful evaluation of the long-term outcome of recent high-dose chemotherapy studies with low-dose radiotherapy for ST-PNET are warranted.

It has recently been suggested that three-dimensional conformal radiotherapy is useful for reducing the dose to the ear structures (28). Intensity-modulated radiotherapy (IMRT) was reported to reduce the dose more, but we must be careful about inducing secondary cancer due to increased whole-body irradiation by IMRT (29). The fact that one patient developed radiation-induced hemangioma in our study showed the importance of reducing unnecessary irradiation in children.

Remarkable advances in molecular biology have led us to routinely use molecular markers to select patients who would be cured with low-dose CSI and those who would respond to chemotherapy. Promeroy et al. have reported that micro-array analysis may be effective for dividing patients with medulloblastoma into favorable and unfavorable groups (30). Gajjar et al. (31) have found a possible relationship between the expression of erbB2 and PFS. Rutkowski et al. (32) have shown that the definitions of favorable and unfavorable risk groups can be improved by the determination of c-myc and trkC mRNA expression. A combined clinical and molecular staging system may well be the breakthrough to accurately predicting disease risk for patients with embryonal tumors in CNS.

The greatest shortcoming of this paper is the small number of patients. Also, combining patients with medulloblastoma and ST-PNET makes it difficult to compare our study with the previous literatures. However, the long-term follow-up of the patients in a single institution has added some potentially important findings. Our experience can be added as supplemental data suggesting a possible role for reduced-dose CSI and chemotherapy in patients with non-metastatic medulloblastoma and ST-PNET.

In conclusion, the combination of surgical resection, ICE chemotherapy and low-dose CSI may have a role in the treatment of a subset of patients with embryonal tumors in the CNS. The possibility of reducing the risk of late neurocognitive damage through reduction of the CSI dose is to be further evaluated.

Funding

Supported by a grain-in-aid from the Japanese Ministry of Education, Culture, Sports, Science, and Technology.

Conflict of interest statement

None declared.

References

1. Freeman CR, Taylor RE, Kortmann R, Carrie C. Radiotherapy for medulloblastoma in children: a perspective on current international clinical research efforts. *Med Pediatr Oncol* 2002;39:99–108.

2. Taylor RE, Bailey CC, Robinson K, Weston CL, Ellison D, Ironside J, et al. Results of a randomized study of preradiation chemotherapy versus radiotherapy alone for nonmetastatic medulloblastoma: the International Society of Paediatric Oncology/United Kingdom Children's Cancer Study Group PNET-3 study. *J Clin Oncol* 2003;21: 1581–91.
3. Gurney JG, Kadan-Lottick NS, Packer RJ, Neglia JP, Sklar CA, Punyko JA, et al. Endocrine and cardiovascular late effects among adult survivors of childhood brain tumors: Childhood Cancer Survivor Study. *Cancer* 2003;97:663–73.
4. Bailey CC, Gnekow A, Wellek S, Jones M, Round C, Brouwn J, et al. Prospective randomized trial of chemotherapy given before radiotherapy in childhood medulloblastoma. International Society of Paediatric Oncology (SIOP) and the (German) Society of Paediatric Oncology (GPO): SIOP II. *Med Pediatr Oncol* 1995;25:166–78.
5. Thomas PRM, Deutsch M, Kepner JL, Boyett JM, Krischer J, Aronin P, et al. Low-stage medulloblastoma: final analysis of trial comparing standard-dose with reduced-dose neuraxis irradiation. *J Clin Oncol* 2000;18:3004–11.
6. Packer RJ, Goldwein J, Nicholson HS, Vezina LG, Allen JC, Ris MD, et al. Treatment of children with medulloblastomas with reduced-dose craniospinal radiation therapy and adjuvant chemotherapy: a Children's Cancer Group Study. *J Clin Oncol* 1999;17:2127–36.
7. Kühl J, Müller HL, Berthold F, Kortmann RD, Deinlein F, Maass E, et al. Preradiation chemotherapy of children and young adults with malignant brain tumors: results of the German pilot trial HIT '88/'89. *Klin Padiatr* 1998;210:227–33.
8. Gentet JC, Bouffet E, Doz F, Tron P, Roche H, Thyss A, et al. Preirradiation chemotherapy including "eight drugs in 1 day" regimen and high-dose methotrexate in childhood medulloblastoma: results of the M7 French Cooperative Study. *J Neurosurg* 1995;82:608–14.
9. Kleihues P, Burger PC, Scheithauer BW. The new WHO classification of brain tumors. *Brain Pathol* 1993;3:255–68.
10. Cohen BH, Zeltzer PM, Boyett JM, Geyer JR, Allen JC, Finlay JL, et al. Prognostic factors and treatment results for supratentorial primitive neuroectodermal tumors in children using radiation and chemotherapy: a Childrens Cancer Group randomized trial. *J Clin Oncol.* 1995;13:1687–96.
11. Reddy AT, Janss AJ, Phillips PC, Weiss HL, Packer RJ. Outcome for children with supratentorial primitive neuroectodermal tumors treated with surgery, radiation, and chemotherapy. *Cancer.* 2000;88:2189–93.
12. Pizer BL, Weston CL, Robinson KJ, Ellison DW, Ironside J, Saran F, et al. Analysis of patients with supratentorial primitive neuroectodermal tumors entered into the SIOP/UKCCSG PNET 3 study. *Eur J Cancer.* 2006;42:1120–8.
13. Allen JC, Donahue B, DaRosso R, Nirenberg A. Hyperfractionated craniospinal radiotherapy and adjuvant chemotherapy for children with newly diagnosed medulloblastoma and other primitive neuroectodermal tumors. *Int J Radiat Oncol Biol Phys.* 1996;36:1155–61.
14. Prados MD, Edwards MS, Chang SM, Russo C, Davis R, Rabbitt J, et al. Hyperfractionated craniospinal radiation therapy for primitive neuroectodermal tumors: results of a Phase II study. *Int J Radiat Oncol Biol Phys.* 1999;43:279–85.
15. Chang CH, Housepian EM, Herbert C. An operative staging system and a megavoltage radiotherapeutic technic for cerebellar medulloblastomas. *Radiology* 1969;93:1351–9.
16. Sawamura Y, Ikeda J, Ishii N, Kato T, Tada M, Abe H, et al. Combined irradiation and chemotherapy using ifosfamide, cisplatin, and etoposide for children with medulloblastoma/posterior fossa primitive neuroectodermal tumor – results of a pilot study-. *Neurol Med Chir (Tokyo)* 1996;36:632–8.
17. Laurent JP, Chang CH, Cohen ME. A classification system for primitive neuroectodermal tumors (medulloblastoma) of the posterior fossa. *Cancer* 1985;56:1807–9.
18. Zeltzer PM, Boyett JM, Finlay JL, Albright AL, Rorke LB, Milstein JM, et al. Metastasis stage, adjuvant treatment, and residual tumor are prognostic factors for medulloblastoma in children: conclusions from the Children's Cancer Group 921 randomized phase III study. *J Clin Oncol* 1999;17:832–45.
19. Packer RJ, Gajjar A, Vezina G, Adams LR, Burger PC, Robertson PL, et al. Phase III study of craniospinal radiation therapy followed by adjuvant chemotherapy for newly diagnosed average-risk medulloblastoma. *J Clin Oncol.* 2006;24:4202–8.
20. Gajjar A, Chintagumpala M, Ashley D, Kellie S, Kun LE, Merchant TE, et al. Risk-adapted craniospinal radiotherapy followed by high-dose chemotherapy and stem-cell rescue in children with newly diagnosed medulloblastoma (St Jude Medulloblastoma-96): long-term results from a prospective, multicentre trial. *Lancet Oncol* 2006;7:813–20.
21. Mulhern RK, Palmer SL, Merchant TE, Wallace D, Kocak M, Brouwers P, et al. Neurocognitive consequences of risk-adapted therapy for childhood medulloblastoma. *J Clin Oncol* 2005;23:5511–9.
22. Goldwein JW, Radcliffe J, Johnson J, Moshang T, Packer RJ, Sutton LN, et al. Updated results of a pilot study of low dose craniospinal irradiation plus chemotherapy for children under five with cerebellar primitive neuroectodermal tumors (medulloblastoma). *Int J Radiat Oncol Biol Phys* 1996;34:899–904.
23. Jakacki RI, Feldman H, Jamison C, Boaz JC, Luerssen TG, Timmerman R. A pilot study of preirradiation chemotherapy and 1800 cGy craniospinal irradiation in young children with medulloblastoma. *Int J Radiat Oncol Biol Phys* 2004;60:531–6.
24. Ris MD, Packer R, Goldwein J, Janes-Wallace D, Boyett JM. Intellectual outcome after reduced-dose radiation therapy plus adjuvant chemotherapy for medulloblastoma: a Children's Cancer Group Study. *J Clin Oncol* 2001;19:3470–6.
25. Palmer SL, Goloubeva O, Reddick WE, Glass JO, Gajjar A, Kun L, et al. Patterns of intellectual development among survivors of pediatric medulloblastoma: a longitudinal analysis. *J Clin Oncol* 2001;19: 2302–8.
26. Grill J, Renaux VK, Bulteau C, Viguier D, Piebois CL, Rose CS, et al. Long-term intellectual outcome in children with posterior fossa tumors according to radiation doses and volumes. *Int J Radiat Oncol Biol Phys* 1999;45:137–45.
27. Oyharcabal-Bourden V, Kalifa C, Gentet JC, Frappaz D, Edan C, Chastagner P, et al. Standard-risk medulloblastoma treated by adjuvant chemotherapy followed by reduced-dose craniospinal radiation therapy: a French Society of Pediatric Oncology Study. *J Clin Oncol* 2005;23:4726–34.
28. Fukunaga-Johnson N, Sandler HM, Marsh R, Martel MK. The use of 3D conformal radiotherapy (3D CRT) to spare the cochlea in patients with medulloblastoma. *Int J Radiat Oncol Biol Phys* 1998;41:77–82.
29. Huang E, Teh BS, Strother DR, Davis QG, Chiu JK, Lu HH, et al. Intensity-modulated radiation therapy for pediatric medulloblastoma: early report on the reduction of ototoxicity. *Int J Radiat Oncol Biol Phys* 2002;52:599–605.
30. Pomeroy SL, Tamayo P, Gaasenbeek M, Sturla LM, Angelo M, McLaughlin ME, et al. Prediction of central nervous system embryonal tumor outcome based on gene expression. *Nature* 2002; 415:436–42.
31. Gajjar A, Hernan R, Kocak M, Fuller C, Lee Y, McKinnon PJ, et al. Clinical, histopathologic, and molecular markers of prognosis: toward a new disease risk stratification system for medulloblastoma. *J Clin Oncol* 2004;22:984–93.
32. Rutkowski S, von Bueren A, von Hoff K, Hartmann W, Shalaby T, Deinlein F, et al. Prognostic relevance of clinical and biological risk factors in childhood medulloblastoma: results of patients treated in the prospective multicenter trial HIT'91. *Clin Cancer Res* 2007;13:2651–7.

Int J Clin Oncol (2008) 13:54–61
DOI 10.1007/s10147-007-0724-4

ORIGINAL ARTICLE

SuYu Zhu · Takashi Mizowaki · Yoshiki Norihisa
Kenji Takayama · Yasushi Nagata · Masahiro Hiraoka

Comparisons of the impact of systematic uncertainties in patient setup and prostate motion on doses to the target among different plans for definitive external-beam radiotherapy for prostate cancer

Received: May 25, 2007 / Accepted: September 11, 2007

Abstract

Background. We aimed to compare the impact of systematic uncertainties in patient setup and prostate motion on three different external-beam radiotherapy protocols for prostate cancer.

Methods. To simulate possible near-maximum systematic errors, the isocenter position was shifted to eight points with ±1.65 SD of the integrated uncertainty value along each axis that was expected to include 5%–95% of the total systematic uncertainties in each direction. Five cases were analyzed for the three plans: an old three-dimensional conformal radiotherapy (3D-CRT) protocol (four-field plus dynamic arc), a new 3D-CRT protocol (dynamic arc), and an intensity-modulated radiotherapy (IMRT) protocol, respectively.

Results. The averaged percentage volume covered by more than 95% of the prescription dose (V95) of the clinical target volume (CTV) for the original plans was 100% for all protocols. After simulating the errors, V95 of the CTV for IMRT cases was maintained at 100%. On the other hand, these values for the new and old 3D-CRT protocols were 93.1% and 63.2%, respectively. The values for the percentage prescription dose received by at least 95% volume (D95) of the CTV for the original plans were 100%, 98.4%, and 97.6% for the IMRT, new 3D-CRT, and old 3D-CRT plans, respectively. However, when the effects of the systematic errors were taken into consideration, the net decreases in the D95 values were 0.3%, 4.3%, and 8.1%, respectively.

Conclusion. The current IMRT protocol is considered to successfully compensate for systematic uncertainties. In contrast, the multi-leaf collimator (MLC) margins set for the old 3D-CRT protocol were not enough to ensure the actual delivery of the prescription dose to the CTV. Therefore, it is very important to include these issues in the plan design in the interpretation of clinical outcomes.

Key words Systematic uncertainties · Dynamic-arc 3D-CRT · IMRT · Prostate cancer

S.Y. Zhu · T. Mizowaki (✉) · Y. Norihisa · K. Takayama · Y. Nagata · M. Hiraoka
Department of Radiation Oncology and Image-applied Therapy, Graduate School of Medicine, Kyoto University, 54 Shogoin-Kawahara-cho, Sakyo, Kyoto 606-8507, Japan
Tel. + 81-75-751-3762; Fax + 81-75-771-9749
e-mail: mizo@kuhp.kyoto-u.ac.jp

Introduction

Geometrical uncertainties in radiotherapy can cause differences between the planned and the actually delivered dose distribution. The uncertainties mainly consist of setup deviation and internal organ motion. Both uncertainties can be separated into random and systematic components.

Setup error and organ motion in external-beam radiotherapy for prostate cancer have been widely investigated using megavoltage film or an electronic portal image device (EPID),[1–3] sequential computed tomography (CT) scans,[4–9] implanted radiopaque markers,[3,10–12] and a B-Mode Acquisition and Targeting System (BAT).[13,14] With better understanding of these uncertainties, the margin added to the clinical target volume (CTV) to create the planning target volume (PTV) is gradually reduced in conformation therapy to reduce the irradiated dose and volume to the organs at risk and to increase the dose to the CTV. However, a PTV margin that is too small will result in geometrical errors at some or even all treatment fractions. It has therefore become increasingly important to quantify and verify whether the applied margins can account for the uncertainties. Among the components of errors, random errors mainly result in blurring the dose distribution.[15,16] This blurring due to the random errors tends to have a relatively small impact on doses to the target and normal structures.[15] On the other hand, systematic errors have a much larger potential to cause significant underdosing or overdosing to both the target and normal structures.[8,15,17]

Therefore, the present study was designed to compare the effect of systematic components of setup errors and prostate motion on prostate dose coverage among three

Table 1. Summary of the three definitive radiotherapy protocols

Protocols	Fields	PTV margins (mm)	MLC and jaw margins (mm)	Setup	Dose (Gy)	Dose prescription
Old 3D-CRT	MLC- Shaped box	Not created	Superior: 12 Inferior: 12 Lateral: 7	Supine without fixation	46	Isocenter
	Dynamic arcs	Not created	Superior: 12 Inferior: 12 Lateral: 7		24	Isocenter
New 3D-CRT	Dynamic arcs	9 (6, Posterior)	Superior: 8 Inferior: 8 Lateral: 3	Supine without fixation	74	Isocenter
IMRT	215° 280° 0° 75° 145°	9 (6, Posterior)	Dynamic MLC, automatic defined: 7–9 mm	Prone with hip fixation	74	D95 of the PTV = 95% (>90%)

PTV, planning target volume; MLC, multi-leaf collimator

definitive external-beam radiotherapy plans for localized prostate cancer, and hence to verify whether the margins set for the three protocols could account for those uncertainties.

Patients, materials, and methods

Description of the three definitive radiotherapy protocols

Since 1998, three definitive radiotherapy protocols have been applied to the treatment of localized prostate cancer at our institute. They are the old three-dimensional conformal radiotherapy (3D-CRT), new 3D-CRT and intensity-modulated radiotherapy (IMRT) protocols, respectively. Details of each planning protocol have already been reported.[18] Briefly, in the old 3D-CRT protocol, a planning target volume (PTV) was not created. A multileaf collimator (MLC) with a leaf width of 1 cm was directly fitted to the clinical target volume (CTV), which is the prostate, with margins. Forty-six Gy in 23 fractions was given, using the four-field box technique with MLC conformation to the CTV, followed by an additional 24 Gy in 12 fractions with the dynamic-arc conformal technique. In the four-field irradiation, MLC or jaw edges were placed directly on the CTV with margins of 12 mm in superior/inferior directions and 7 mm in the remaining directions based on the beam's eye view of each field. If a part of the posterior rectal wall was included in the lateral opposing fields, the MLC positions were manually adjusted to completely shield the posterior wall from the irradiated area by the bilateral fields. In the dynamic-arc conformal radiotherapy, two lateral arcs with 100° of rotation (from 36° to 136°, and from 226° to 326°) were used with dynamic conformal fitting of MLCs to the CTV with a 7-mm margin. In the new 3D-CRT and IMRT protocols, PTV was created by adding a 9-mm margin to the CTV, except for the posterior rectal-prostate interface, where a 6-mm margin was applied. For the new 3D-CRT protocol, two lateral dynamic arcs with 100° of rotation (from 36° to 136° and from 226° to 326°) were used by dynamic conformal fitting of MLCs to the PTV, in which a 3-mm margin was generally placed from the edge of the PTV to the tips of the MLCs. With respect to the superior and inferior directions, jaws were fitted with an 8-mm margin to the PTV to ensure 95% dose at the edge of the PTV. For the IMRT protocol, inverse optimization was used to achieve the goal that the percentage prescription dose received by at least 95% volume (D95) of the PTV should generally exceed 95% (at least 90%). The old and new 3D-CRT techniques are performed with the patients in the supine position without any fixation, while IMRT is applied with the patients immobilized in the prone position, using thermoplastic shells fixed to a rigid pelvic board Hip Fix (MedTec, Inc, Orange City, IA, USA) extending from the mid-thigh to the upper third of the leg and with the feet being put on a cushion support. Details of the three protocols are summarized in Table 1.

Institutional measured uncertainties

From March 2001 to March 2002, a study was conducted to measure setup errors and prostate motion using serial computed tomography (CT) verification scans. Ten patients in the supine position, without fixation devices, and eight patients in the prone position, fixed with a set of thermoplastic shells, were enrolled in the study. Three CT verification scans were performed at 2-week intervals for the whole course of radiotherapy for each patient. CT scans were conducted with the same conditions as the simulation scans; that is, empty rectum and moderately dilated bladder (0.5–1.0 h after micturition). The three serial CT scan images were registered to the simulation CT scan images using the same Digital Imaging and Communications in Medicine (DICOM) coordinates. The prostate was contoured and the center was reconstructed. Four reference points on the pelvic bony structure (two on the innermost edge of the femoral head, one on the anterior-superior edge of the coccyx, and one on the posterior-superior edge of the pubic symphysis) were chosen to calculate the relative position of the prostate along three axial directions. Compared with the relative prostate position on the simulation CT images, the systematic and random prostate motions were calculated. The systematic displacement was taken to be the difference between the prostate position in the planning scan and the mean position as calculated from the three treatment scans, and the random displacements were calculated as the devia-

Table 2. Institutional data of systematic uncertainties and the integration used for simulations

	1 SD of systematic setup error	1 SD of systematic prostate motion	1 SD of integrated systematic error ($\Sigma\delta^2 = IM^2 + SM^2$)	Simulating value 1.65 SD (5%–95% CI)
	Prone Supine	Prone Supine	Prone Supine	Prone Supine
LR (mm)	1.6	0.8	1.8	3.0
	3.0	0.9	3.1	5.1
AP (mm)	1.6	2.1	2.6	4.3
	3.4	3.7	5.0	8.3
CC (mm)	3.1	3.1	4.4	7.3
	3.2	1.7	3.6	5.9

LR, Left-right; AP, anterior-posterior; CC, cranial-caudal; δ, total margin; IM, internal margin; SM, setup margin; CI_c confidence interval

tion of the prostate position in each treatment scan from the mean position. Thus, one systematic and three random displacements were calculated for each patient. Regarding the whole study cohort, the SD for the systematic error was assessed as the SD of the ten patients in the supine position or the eight patients in the prone position. The SD for the random error was taken as the SD of 30 random displacements in the supine position or 24 in the prone position for the ten or eight patients, respectively. The differences between simulation and treatment CT coordinate positions of the center of the four pelvic bony reference points along three axes were, accordingly, calculated as the axial setup errors; the SD values of systematic errors are displayed in Table 2.

Isocenter shifting model simulating systematic setup errors and prostate motion

Integration of the systematic errors of the setup and internal prostate motion

The International Commission on Radiation Units and Measurements (ICRU) report 62 discussed several scenarios about how to composite the internal margin (IM) with the setup margin (SM). The report recommended creating a "global" safety margin to be adopted by means of the quadrature formalism ($\Sigma\delta 2 = IM2 + SM2$) in a quantitative approach.[18] According to the recommendation, we integrated setup errors and organ motions because the simple linear addition of two kinds of error would lead to an excessively large integrated systematic error. The calculated values of integrated systematic errors along the three axes are indicated in Table 2, for the supine and prone positions separately.

Representative shifting value of 1.65 SD along each of the three Cartesian directions

We assume that the prostate motions and setup errors can each be described by three orthogonal independent Gaussian (normal) distributions. This is a reasonable assumption, because several groups have proved that the data are normally distributed.[4,7,10,20] In this case, the calculated integrated systematic uncertainties should also be in normal distribution. Therefore, 90% (5% to 95%) of the systematic uncertainties are included within ±1.65 SD. This is because, if we consider a patient group as a whole, the mean value of the systematic errors would be very close to zero, as indicated in our institutional results. Therefore, in this study, we chose 1.65 SD of the integrated systematic uncertainties on each of the three axes, which was expected to cover 90% of the systematic isocenter shifts in each direction.

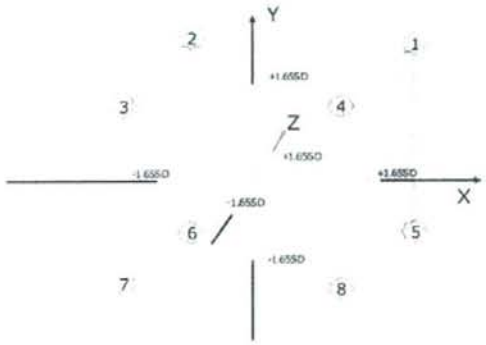

Fig. 1. Isocenter shifting model: ±1.65 SD was first chosen as the coordinate for axial check points (three pairs). Based on the six axial check points, eight vector combination points were created. The eight corner points were the worst-case scenario within a ±1.65 SD axial value

Simulating the impacts of the systematic errors on the dose distribution

To simulate the impacts of possible large systematic errors on the dose distribution, we shifted the isocenter to the eight points with +/–1.65 SD value on each axis (vector combination points; Fig. 1).

The isocenter shifting was conducted on five IMRT plans in the prone position with hip fixation, and on five new 3D-CRT plans in the supine position without fixation, and on

the old 3D-CRT plans created using the new 3D-CRT patients' contoured images strictly complying with the protocols. To further compare the new 3D-CRT protocol with the IMRT protocol, the five new 3D-CRT plans were created based on the respective CT data set for IMRT plans in the prone position with fixation devices complying with the planning protocol accordingly. The same magnitude of systematic uncertainties in the prone position with the fixation device was applied to simulate shifting the isocenter. All the created plans were checked and were approved by our department board. Shifted plans were created and dose distributions were recalculated. In total, 160 shifted plans were created and statistical data were collected and analyzed.

Analyses based on dose volume histogram (DVH) data

With the Eclipse treatment planning system (Varian Medical Systems, Inc., Palo Alto, CA, USA), the DVHs of the PTV and the CTV (prostate) were calculated for the original plans and the total shifted plan. The total shifted plan was defined as the plan with the averaged dose distribution of the eight shifted plans for each case. Therefore, the total shifted plan was considered to be the plan reflecting the averaged effect of the simulated systematic uncertainties. For the PTV and CTV, the percentage volume covered by more than 95% of the prescription dose (V95) and the percentage prescription dose received by at least 95% volume (D95) were calculated. In addition, minimal, maximal, and mean percent doses were collected for analyses. The dose conformity to the PTV was calculated using the conformity index (CI) equation advocated by Van't Riet et al.[21] The CI is defined as the product of the fraction of the PTV receiving at least 95% of the prescription dose and the ratio of the volume of the PTV receiving at least 95% of the prescription dose to the body volume receiving at least 95% of the prescription dose, which is indicated by the following equation:

$$\text{Conformity index (CI)} = \text{VPTV95\%/VPTV} * \text{VPTV95\%/Vt}$$

Here, VPTV95% is the PTV volume covered by 95% of the prescription dose, VPTV is the volume of the PTV, and Vt is the body volume covered by 95% of the prescription dose. Therefore, the CI accounts for both any normal tissue volume receiving at least 95% of the prescription dose and for any volume of the PTV receiving less than 95% of the prescription dose. For the new and old 3D-CRT plans, because the same patients' images and systematic uncertainties for simulations of isocenter shifting were applied, comparisons of the DVHs for the same PTV and CTV were made. New 3D-CRT plans created on the CT data sets in the prone position were also compared to the corresponding IMRT plans with respect to the DVH indexes. The DVHs for the shifted plan for each case were calculated using a summed plan function with the same weight assigned to each single shift. The mean DVHs both for the original and shifted plans for each protocol were calculated by averaging their corresponding percentage volume at the same incremental dose steps. The P value was calculated by the two-tailed paired Student's t-test.

Results

Table 3 and Table 4 show the planning results of the PTV and CTV for five cases using the three respective protocols. The V95 and D95 values of the CTV for the three protocols were almost comparable ($P > 0.05$) and the differences in the other indexes among the three protocols were also small. However, when the same PTV definition as for the new 3D-CRT and IMRT protocols was applied to the old 3D-CRT protocol, the V95, D95, mean dose, and CI for the old 3D-CRT cases were greatly inferior to those for the cases with the other two protocols ($P < 0.001$), indicating

Table 4. RTP results for CTV with the three protocols

	IMRT (mean ± SD)	New 3D-CRT (mean ± SD)	Old 3D-CRT (mean ± SD)
V95 (%)	100 ± 0	100 ± 0	99.9 ± 0.1
D95 (%)	100 ± 0.9	98.4 ± 0.7	97.6 ± 0.6
Minimum dose (%)	98.1 ± 1.2	97 ± 0.6	95.3 ± 1.1
Maximum dose (%)	108.3 ± 1.8	102.6 ± 0.4	101.2 ± 0.5
Mean dose (%)	103.7 ± 0.7	100.7 ± 0.7	99.6 ± 0.3

V95, Percent target volume receiving 95% of the prescription dose or higher; D95, percent prescription dose covering 95% of the target volume

Table 3. RTP results for PTV with the three protocols

	IMRT (mean ± SD)	New 3D-CRT (mean ± SD)	Old 3D-CRT (mean ± SD)
V95 (%)	99 ± 0.5	93.9 ± 0.9	59.6 ± 6.8
D95 (%)	97 ± 0.5	94.5 ± 0.3	82.9 ± 1.5
Minimum dose (%)	87.7 ± 4.8	87.5 ± 0.7	60 ± 3.3
Maximum dose (%)	108.5 ± 1.8	102.6 ± 0.4	101.3 ± 0.5
Mean dose (%)	102.3 ± 0.7	99.5 ± 0.3	94.9 ± 1
Conformity index	0.88 (0.87–0.89)	0.76 (0.72–0.78)	0.60 (0.52–0.65)

V95, Percent target volume receiving 95% of the prescription dose or higher; D95, percent prescription dose covering 95% of the target volume; conformity index = $V_{PTV95\%}/V_{PTV}$* $V_{PTV95\%}/Vt$ [a]
For conformity index: mean (range)

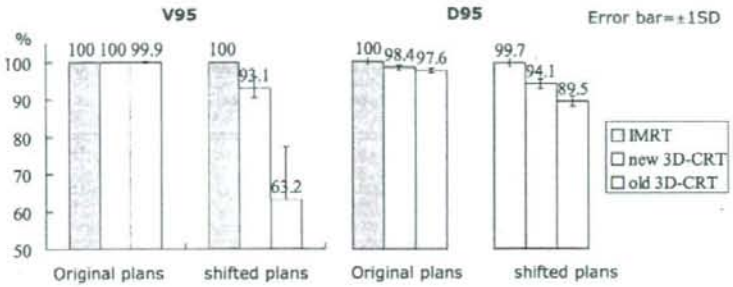

Fig. 2. Mean percent target volume receiving 95% of the prescription dose or higher (*V95*) and percent prescription dose covering 95% of the target volume (*D95*) for dose volume histogram (DVH) of the clinical target volume (CTV) of the three protocols before and after taking systematic uncertainties into consideration. *Error bar*, ±1 SD. *MRT*, modulated radiotherapy; *3D-CRT*, three-dimensional conformal radiotherapy

the original MLC margins set for this protocol are insufficient if the dose evaluation is based on the current PTV concept. The CI for the IMRT plans was the highest among the three protocols, which indicates the dose distributions in the IMRT plans conform best to the PTV compared to those in the new and old 3D-CRT plans.

Figure 2 indicates the V95 and D95 of the CTV for the original plans and the simulated isocenter-shifted plans. The V95s for all three protocols were excellent and reached 100% of the prescribed dose, while D95 values were also 97% or higher for all protocols. On the other hand, although the averaged V95 for total shifted IMRT plans was maintained at 100%, those for the new 3D-CRT and old 3D-CRT plans decreased to 93.1% and 63.2%, respectively. The decreasing rate of the V95 values for the old 3D-CRT cases was most evident compared with those for the other two protocol's cases. The same trend as for V95 was observed with respect to D95, although the magnitudes of the deterioration after simulating the systematic uncertainties in the old 3D-CRT cases were relatively smaller than those for the V95. The net decrease for IMRT cases was minimum (0.3%), while that for the old 3D-CRT cases was the biggest (8.1%) among the three protocols.

Figure 3 indicates the mean DVHs of the CTV for the original and total shifted plans of the three protocols. For the IMRT protocol, the two curves almost coincided with each other. Compared with the original new 3D-CRT plans, definitive insufficient dose coverage was observed with respect to the total shifted plans. Again here, the worsening of the CTV dose coverage for the old 3D-CRT plans was the most marked among the protocols. The detailed net decreases in the DVH statistics of the CTV after simulating the systematic uncertainties are indicated in Table 5.

The mean DVH of the CTV for the new 3D-CRT plans created on the CT data sets for the IMRT protocol is shown in Fig. 4. The net decreases in the V95, D95, minimum dose, maximum dose, and the mean dose for the IMRT protocol, the new 3D-CRT protocol, and the new 3D-CRT plans created on the CT data sets scanned in the prone position are indicated in Fig. 5. Although the net decreases in the V95, D95, minimum dose, maximum dose, and mean dose became much smaller when the new 3D-CRT plans were created with the patients in the prone position with hip fixation than when created with the patients in the supine

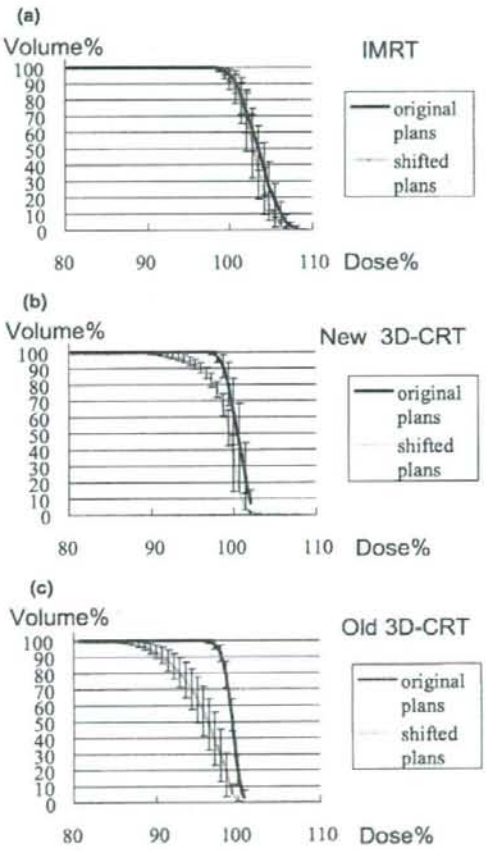

Fig. 3a–c. Mean DVH of the CTV before and after taking systematic uncertainties into consideration, for IMRT (**a**), new 3D-CRT (**b**), and old 3D-CRT protocols (**c**). *Error bar*, ±1 SD

Table 5. Comparison of the net decreases in the DVH statistics of the CTV for the three protocols after simulation of systematic uncertainties

	IMRT		New 3D-CRT		Old 3D-CRT	
	Net decrease (%)	*P* value	Net decrease (%)	*P* value	Net decrease (%)	*P* value
V95	0	0.4	6.9	0.005	36.7	0.004
D95	0.3	0.02	4.3	0.001	8.1	<0.0001
Min.	2.4	0.1	8.3	0.0001	11.8	<0.0001
Max.	1.7	0.003	1	0.006	1.3	0.003
Mean	0.7	<0.0001	1.5	0.0007	3.7	0.0008

V95, Percent target volume receiving 95% of the prescription dose or higher; D95, percent prescription dose covering 95% of the target volume

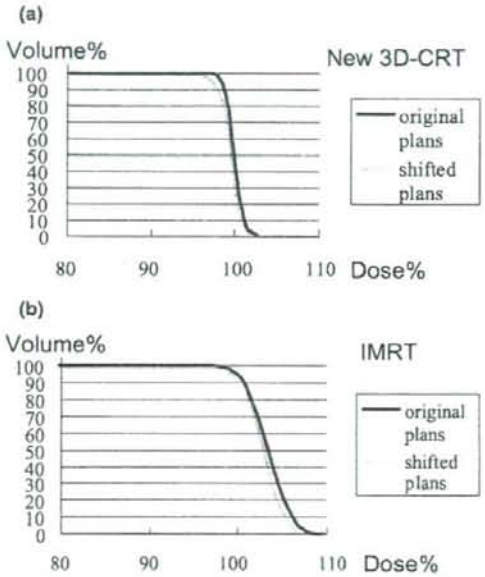

Fig. 4a,b. Comparison of the mean DVH of the CTV, for the new 3D-CRT (**a**) and IMRT plans (**b**) before and after taking systematic uncertainties into consideration based on the same condition: new 3D-CRT plans were created on the IMRT plan images and the systematic uncertainties of the prone position with hip fixation were simulated for the two protocol plans

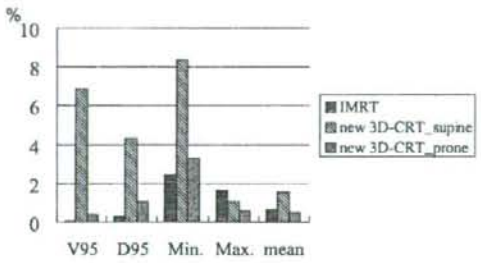

Fig. 5. Net decrease in the DVH indexes of the CTV for IMRT, new 3D-CRT_supine, and new 3D-CRT_prone plans after taking systematic uncertainties into consideration. *New 3D-CRT_supine* represents the new 3D-CRT plans simulating the systematic uncertainties in the supine position without using an immobilization device. *New 3D-CRT_prone* represents the new 3D-CRT plans created based on the IMRT plan images simulating the systematic uncertainties in the prone position with hip fixation

position without fixation, the IMRT plans still had some advantages in terms of target coverage.

Discussion

The ICRU report 50[27] recommends defining a geometrical structure of PTV to compensate for the effect of uncertainties. The magnitude of PTV can predict and project the potential location of the CTV. Margins to create the PTV from the CTV (PTV margin) should take into account both setup errors and internal organ motion. However, in most cases, the CTV is often located adjacent to the organs at risk (OARs), which prevents us from using margins large enough to cover all of the uncertainties for most patients. Therefore, adequate margins to compensate for 90%–95% of the uncertainties should be used to create the PTV. More importantly, the magnitude of the adequate margin is also influenced by the method of patient fixation or error reduction strategies. To see whether the defined margins account for the uncertainties, we examined and compared the adequacy of three definitive radiotherapy protocols for localized prostate cancer, in terms of the CTV coverage, by simulating possible large systematic errors with respect to patient setup and internal organ motion.

In the present study, several assumptions were made, based on the previously published literature; we assumed that random errors have a relatively smaller impact on the dose distribution to the prostate,[15–17] while systematic errors are in normal distribution.[4,7,10,20] Because our purpose was to compare planning strategies of three different radiotherapy protocols and to estimate their validity by verifying the tolerability in CTV coverage, we only simulated systematic

errors. To include all the possible systematic uncertainties, it would be necessary to apply nearly ±3 SD. However, we carefully chose ±1.65 SD of the systematic error as a checkpoint value for the isocenter shift, which includes 90% (from 5% to 95%) systematic uncertainties along each axis. Therefore, there were in total eight check points (Fig. 1). With these check points, we expected to include most of the possible systematic displacements while excluding very extreme shifts, which is reasonable for comparing the adequacy among different radiotherapy protocols.

Our previous study showed that the dynamic-arc 3D-CRT (new 3D-CRT) could achieve a comparable dose distribution to that achieved with IMRT with respect to the target coverage and rectal sparing in external-beam radiotheapy for localized prostate cancer with a prescription dose of 74 Gy. On the other hand, the old 3D-CRT plan could not reach a qualified dose coverage for the target, based on the current PTV concept, due to the universally smaller portal margins applied.[18] This continuing study shows that when the systematic uncertainties were incorporated into the dose distribution analyses, the difference between the planned and the actually delivered target dose was much larger for the old 3D-CRT plan, and a detectable dose decrease also appeared in the dynamic-arc 3D-CRT plan. However, the IMRT plan still maintained an intended target coverage of the prostate (CTV). Therefore the IMRT protocol is considered to be superior to the dynamic-arc 3D-CRT plan in terms of tolerability against systematic uncertainties.

A big question here is what are the adequate acceptance criteria with respect to the dose decrease from the planned to the actually delivered dose supposing the random factors could be neglected. The answer could not be drawn from the literature. van Herk[17] discussed this point in his review article and analyzed several examples, but the criteria were diverse and could not be uniformly applied: they should be institution-dependent and also treatment-technique-dependent. A general guideline for the target coverage in traditional static dose distribution is reported in ICRU report 50,[22] where the PTV should guarantee that 95% of the prescription dose is delivered to at least 90% of the CTV. Based on this guideline, the actually delivered dose distribution with the old 3D-CRT plans is unacceptable, which means margins applied directly to the CTV and simply defined by jaws/MLCs are universally insufficient to account for systematic uncertainties. However, the difference between the planned and actually delivered dose distribution to the CTV with IMRT plans is nominal, indicating that the margins set successfully compensate for the systematic uncertainties.

There are two main reasons why the ability to account for the systematic uncertainties between our IMRT and the new 3D-CRT protocol plans is different. One is patient position-related and immobilization-related uncertainty values, and the other is the treatment techniques themselves, which define dose conformity to, and the dose gradient from, the PTV. A comparison of the effect of the systematic uncertainties on the new 3D-CRT plans and the IMRT plans based on the same image pool simulating the same values of uncertainties, resulted in the slight superiority of the IMRT protocol to the new 3D-CRT protocol to account for the systematic uncertainties. At the same time, we also noticed that the degree of decrease in dose coverage after simulating the systematic uncertainties for the new 3D-CRT plans was much smaller when the patients were fixed in the prone position and immobilized with hip fixation than when they were treated in the supine position without any fixation devices. This may indicate that if, for our new 3D-CRT protocol, we also immobilize patients in the prone position with hip fixation, as is done with the patients receiving the IMRT protocol, we may get much better actual dose distribution. It has been reported that the prostate movement in the prone position was much larger that that in the supine position if no fixation devices were used, probably because of the effect of respiration.[11] Therefore, it is strongly recommended that we should use a fixation device when treating patients in the prone position.

There were some remarks in the literature that the IMRT was more sensitive to uncertainties than 3D-CRT due to its sharper dose gradients in the peripheral region of the PTV. Our data show that this is not necessarily true. The sensitivity to treatment-related uncertainties strongly depends on the given margins for the PTV and the error reduction strategies applied, as well as the degree of dose fall-off outside the PTV.

One drawback of the present study was that the effect of systematic uncertainties on the doses to the rectum and bladder was not incorporated into the dose distribution analyses of the target. The original planned dose range to the rectum and bladder was large, and rectum filling was diverse; all these factors make the incorporation much more complicated. Therefore, we believe a deformable image registration technique should be incorporated in the treatment planning based on a 4D imaging data set in the future.

In conclusion, differences in the CTV dose among three protocols for definitive external-beam radiotherapy when systematic uncertainties were taken into consideration were evaluated. Our current IMRT protocol, with fixation devices used in the prone position, was considered to successfully compensate for decreased systematic uncertainties, while the old 3D-CRT protocol was inadequate to realize an adequate CTV dose, although the CTV dose was sufficient in terms of the static protocol data. In the future, a 4D dataset-based method for radiotherapy protocol evaluation will be necessary to accurately estimate the actually delivered dose to the targets and organs at risk.

Acknowledgments This study was supported in part by a Grant-in-Aid for Scientific Research on Priority Areas Cancer from the Ministry of Education, Culture, Sports, Science and Technology of Japan (No. 17016036), and a Grant-in-Aid for Scientific Research from the Ministry of Education, Culture, Sports, Science and Technology of Japan (No. 16659316 and 17390333).

References

1. Bijhold J, Lebesque JV, Hart AA, et al. (1992) Maximizing setup accuracy using portal images as applied to a conformal boost technique for prostatic cancer. Radiother Oncol 24:261–271

2. Hurkmans CW, Remeijer P, Lebesque JV, et al. (2001) Setup verification using portal imaging: review of current clinical practice. Radiother Oncol 58:105–120
3. Vigneault E, Pouliot J, Laverdiere J, et al. (1997) Electronic portal imaging device detection of radioopaque markers for the evaluation of prostate position during megavoltage irradiation: a clinical study. Int J Radiat Oncol Biol Phys 37:205–212
4. Antolak JA, Rosen II, Childress CH, et al. (1998) Prostate target volume variations during a course of radiotherapy. Int J Radiat Oncol Biol Phys 42:661–672
5. Beard CJ, Kijewski P, Bussiere M, et al. (1996) Analysis of prostate and seminal vesicle motion: implications for treatment planning. Int J Radiat Oncol Biol Phys 34:451–458
6. Lattanzi J, McNeely S, Hanlon A, et al. (1998) Daily CT localization for correcting portal errors in the treatment of prostate cancer. Int J Radiat Oncol Biol Phys 41:1079–1086
7. Roeske JC, Forman JD, Mesina CF, et al. (1995) Evaluation of changes in the size and location of the prostate, seminal vesicles, bladder, and rectum during a course of external beam radiation therapy. Int J Radiat Oncol Biol Phys 33:1321–1329
8. Stroom JC, Koper PC, Korevaar GA, et al. (1999) Internal organ motion in prostate cancer patients treated in prone and supine treatment position. Radiother Oncol 51:237–248
9. Zelefsky MJ, Crean D, Mageras GS, et al. (1999) Quantification and predictors of prostate position variability in 50 patients evaluated with multiple CT scans during conformal radiotherapy. Radiother Oncol 50:225–234
10. Balter JM, Sandler HM, Lam K, et al. (1995) Measurement of prostate movement over the course of routine radiotherapy using implanted markers. Int J Radiat Oncol Biol Phys 31:113–118
11. Kitamura K, Shirato H, Seppenwoolde Y, et al. (2002) Three-dimensional intrafractional movement of prostate measured during real-time tumor-tracking radiotherapy in supine and prone treatment positions. Int J Radiat Oncol Biol Phys 53:1117–1123
12. Wu J, Haycocks T, Alasti H, et al. (2001) Positioning errors and prostate motion during conformal prostate radiotherapy using on-line isocentre setup verification and implanted prostate markers. Radiother Oncol 61:127–133
13. Little DJ, Dong L, Levy LB, et al. (2003) Use of portal images and BAT ultrasonography to measure setup error and organ motion for prostate IMRT: implications for treatment margins. Int J Radiat Oncol Biol Phys 56:1218–1224
14. Trichter F, Ennis RD (2003) Prostate localization using transabdominal ultrasound imaging. Int J Radiat Oncol Biol Phys 56: 1225–1233
15. Bortfeld T, Jiang SB, Rietzel E (2004) Effects of motion on the total dose distribution. Semin Radiat Oncol 14:41–51
16. Levitt SH, Khan FM (2001) The rush to judgment: does the evidence support the enthusiasm over three-dimensional conformal radiation therapy and dose escalation in the treatment of prostate cancer? Int J Radiat Oncol Biol Phys 51:871–879
17. van Herk M (2004) Errors and margins in radiotherapy. Semin Radiat Oncol 14:52–64
18. Zhu S, Mizowaki T, Nagata Y, et al. (2005) Comparison of three radiotherapy treatment planning protocols of definitive external-beam radiation for localized prostate cancer. Int J Clin Oncol 10:398–404
19. International Commission on Radiation Units and Measurements (1999) ICRU Report 62: prescribing, recording, and reporting photon beam therapy (supplement to ICRU report 50). Oxford University Press, Oxford
20. Rudat V, Schraube P, Oetzel D, et al. (1996) Combined error of patient positioning variability and prostate motion uncertainty in 3D conformal radiotherapy of localized prostate cancer. Int J Radiat Oncol Biol Phys 35:1027–1034
21. van't Riet A, Mak AC, Moerland MA, et al. (1997) A conformation number to quantify the degree of conformality in brachytherapy and external beam irradiation: application to the prostate. Int J Radiat Oncol Biol Phys 37:731–736
22. International Commission on Radiation Units and Measurements (1993) ICRU Report 50: prescribing, recording, and reporting photon beam therapy. Oxford University Press, Oxford

肺癌
―照射野決定のための画像診断のポイントと効果判定・経過観察の注意点―

永田 靖*, **　澁谷景子*　松尾幸憲*　山内智香子*
小倉健吾*　平岡真寛*

肺癌の病期診断では，正確なTNM分類を行うために，肺内小腫瘤，脳内小腫瘤，副腎内腫瘤，骨腫瘤，リンパ節の診断が重要である．また，治療効果判定においては腫瘍の最大縮小時期の見極めが，再発判定においては放射線肺臓炎と残存腫瘤との鑑別が重要である．

はじめに

"放射線治療のための画像診断"とは，言い換えると"放射線治療医の求める画像診断レポート"と言えよう．そして"放射線治療に必要な画像診断"とは，1) 正確な病期診断，2) 適切な治療効果判定，3) 迅速な再発診断の3点に集約できよう．

一般に画像診断は大きく分けて，

1) 存在診断（病気があるかないか?）
2) 性状診断（悪性か良性か?）
3) 進展診断（どこまで病気が進展しているか?）

に分類できる．このなかで，放射線治療において大部分は，既に癌であることが組織学的に確定している疾患や病変を治療対象としているために，上記の3) の進展診断が最も重要である．しかし，後述する理由により，2) の性状診断もまた非常に重要である．また，放射線治療は，最大効果出現の時期が疾患や部位，組織型により異なる．そのために，適切な時期に最適な画像診断法で効果判定を行うことが重要である．これに密接に関連して，放射線治療後の残存瘢痕と再発診断が臨床上では非常に重要となる．

本稿では，肺癌に特化して以上の項目について検討したい．

肺癌は，年間約3万人の患者が放射線治療を受け，放射線治療対象のなかで最も多い疾患のひとつである．このなかにはI期早期肺癌に対する定位（ピンポイント）放射線照射[1]，II～III期肺癌に対する根治的化学放射線治療，IV期肺癌（骨転移，肺転移，上大静脈症候群）に対する緩和照射が含まれる．

1. 正確な病期診断

まず，病変がどこまで進展しているかによって治療方針が大きく異なる．これを規定するものがいわゆるTNM分類である．治療前に正確なTNM分類が行われて初めて最適な治療法の選択が可能となる．

肺癌のTNM分類は，表に示すとおりである．

T分類において，現在は腫瘍サイズが最大径3cmあるかないかでT1とT2とが区別されている．しかし，2009年の国際対癌連合（UICC）のTNM分類の大改訂では，2cm，3cm，5cm，7cmでT分類が変わることになる予定である[2]．

また，T分類においては主病変以外の組織未定の肺野の小結節評価が非常に重要である．肺野の単発病変ともう1か所病変があることによって，これを転

* Nagata Y., Shibuya K., Matsuo Y., Yamauchi C., Ogura K., Hiraoka M.　京都大学医学部放射線治療科　**現）広島大学病院放射線治療部

表　肺癌のTNM分類

原発腫瘍（T）
- T1：腫瘍の最大径は3.0cmまたはそれ未満の大きさで，肺または臓側胸膜に囲まれており，気管支鏡検査で浸潤が葉気管支より中枢側に及ばない．
- T2：腫瘍の大きさや進展度が以下のいずれかのもの．
  - 最大径が3cmを超えるもの．
  - 主気管支に浸潤し，気管分岐部より2.0cmあるいはそれより末梢にある．
  - 臓側胸膜に浸潤．
  - 肺門に及ぶが片肺全野には及ばない無気肺あるいは閉塞性肺臓炎に関連する．
- T3：大きさと無関係に隣接臓器，すなわち胸壁［肺尖部胸壁浸潤肺癌（superior sulcus tumor）を含む］，横隔膜，縦隔胸膜，壁側心膜などに直接浸潤する腫瘍．腫瘍の中枢側が気管分岐部より2.0cm未満に及ぶが，気管分岐部に浸潤のないもの．また，無気肺・閉塞性肺臓炎が片肺全野に及ぶもの．
- T4：大きさと無関係に次のどれかに浸潤の及ぶ腫瘍．
  - 縦隔，心臓，大血管，気管，食道，椎体，気管分岐部．
  - あるいは同一肺葉内の離れた腫瘍．
  - あるいは悪性胸水を伴う腫瘍．

所属リンパ節（N）
- N0：所属リンパ節に転移がない．
- N1：同側気管支周囲と同側肺門リンパ節転移の少なくとも一方，そして肺腫瘍の直接進展を含む肺内リンパ節転移．
- N2：同側縦隔と気管分岐部リンパ節転移の少なくとも一方．
- N3：対側縦隔，対側肺門，同側または対側の斜角筋前，あるいは鎖骨上リンパ節転移．

遠隔転移（M）
- M0：遠隔転移がない．
- M1：遠隔転移がある．

移とすれば，T1がT4ないしはM1に大きく変化することになる．もし，これが肉芽腫ならT1N0M0のままである．つまり，根治の望めるT1N0M0ならば手術や体幹部定位照射が可能である．しかし，T1N0M1では化学療法か緩和医療の対象となり，治療方針が大きく異なることになる．以上の点より，画像診断レポート作成時に組織診断の確定していない肺野の小結節については，診断に注意が必要である．明確な根拠なしに肺内転移と診断すると，患者が治癒のチャンスを失う可能性があるためである．図1は，組織診断のつかなかった次第に拡大する肺腫瘤の1例である．

また，現在の保険診療上で，肺転移腫瘍に対して3か所以内なら定位放射線照射が適応となる．仮に，4か所以上の腫瘍なら化学療法の対象となる．腫瘍が3個か4個かで大きく治療方針が異なってくる事例である．肺野の小腫瘤の診断が治療方針に大きく影響し，画像診断レポートにおいて「多発転移」のみでは，臨床判断には不十分な理由である．

T分類において壁側胸膜に浸潤しているかについては，4次元動画CTも有用である．

次にN分類におけるリンパ節転移についても，癌

CT（肺野条件）

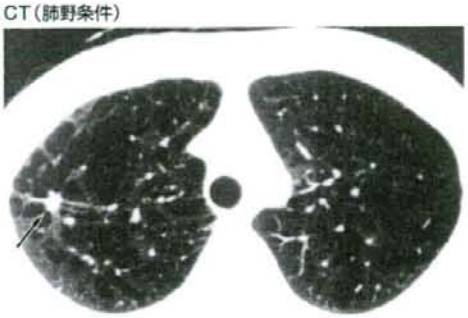

図1　組織型の確認できなかった次第に拡大してくる孤立性肺腫瘤
臨床的に肺癌とされ体幹部定位照射が行われた（→）．

の転移以外に炎症性腫脹やサルコイド反応（図2）があることは言うまでもない．サルコイド反応であっても照射でリンパ節は縮小する．最終的には縦隔鏡で確定しなければ，縦隔リンパ節転移の確定は難しい．

最後にM分類について検討すると，図3は左副腎に単発性の肺癌転移が疑われた症例であるが，最終

A CT(上から下へ順番)

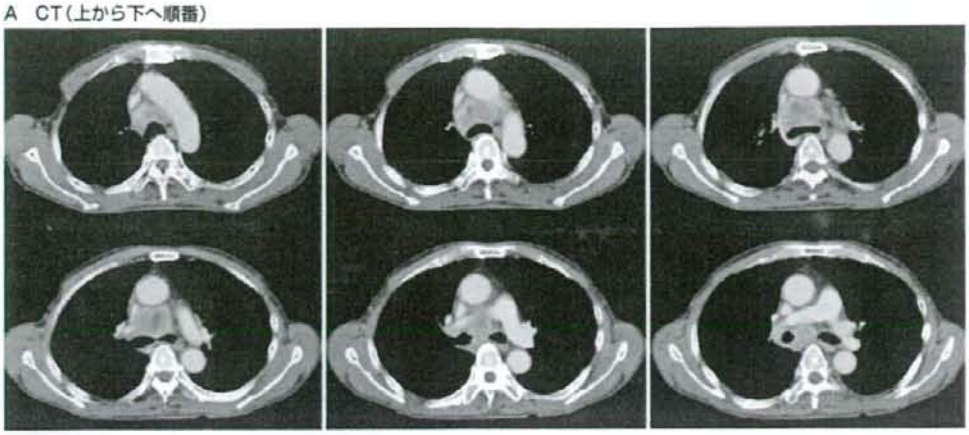

B CT

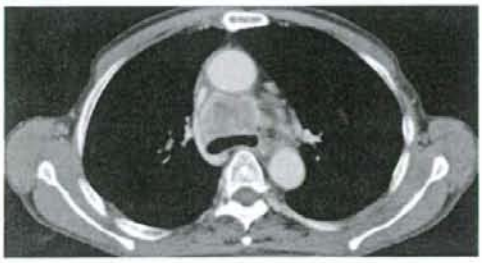

図2 肺癌による縦隔リンパ節転移疑い
A, B：肺癌による縦隔リンパ節転移が強く疑われたが，縦隔鏡組織検査ではサルコイド反応のみであった．

A CT

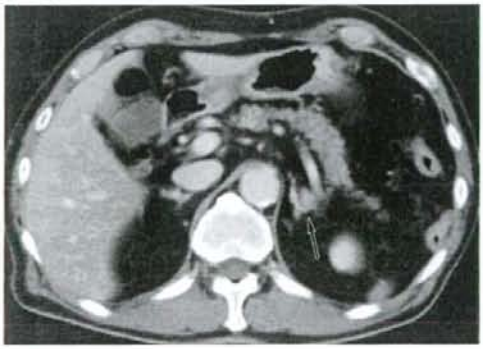

B CT

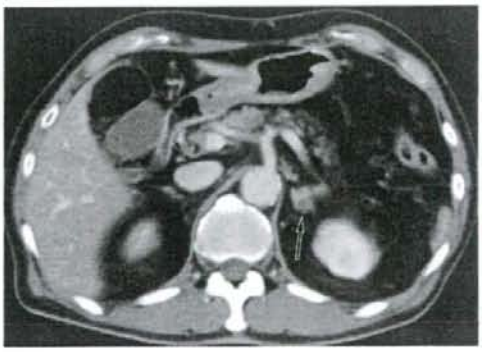

図3 60歳代，男性 左副腎転移疑い
A, B：副腎転移（→）が疑われた症例であるが，臨床経過から見て，最終的に副腎腺腫とされた．

的には副腎は良性の腺腫となった．その結果，患者は肺癌の根治的定位照射を受けることになった．

同様に脳転移腫瘍も組織型の確認なしに，画像診断と臨床経過とを根拠として治療されることがほとんどである．図4の症例も脳転移として紹介されたが，最終診断はMR画像上のアーチファクト症例であり，脳定位照射の適応にはならなかった．このように，組織診断の確認されていない腫瘍の診断には細心の注意が必要である．

骨転移においても，骨転移と鑑別困難な変形性脊